Entanglement in quantum catastrophes

Clive Emary*
Instituut-Lorentz, Universiteit Leiden, P.O. Box 9506, 2300 RA Leiden, The Netherlands

Neill Lambert and Tobias Brandes
School of Physics and Astronomy, The University of Manchester, P.O. Box 88, Manchester M60 1QD, United Kingdom
(Received 17 March 2005; published 6 June 2005)

We classify entanglement singularities for various two-mode bosonic systems in terms of catastrophe theory. Employing an abstract phase-space representation, we obtain exact results in limiting cases for the entropy in cusp, butterfly, and two-dimensional catastrophes. We furthermore use numerical results to extract the scaling of the entropy with the nonlinearity parameter, and discuss the role of mixing entropies in more complex systems.

DOI: 10.1103/PhysRevA.71.062302 PACS number(s): 03.67.Mn, 03.65.Ud, 42.50.Fx

I. INTRODUCTION

For a large number of quantum critical systems, criticality manifests itself as a peak, or indeed a divergence, in the entanglement of the ground state. Systems in which this behavior has been observed include spin-$1/2$ ferromagnetic chains in a magnetic field [1], driven, dissipative large-j pseudo-spin models [2], the Lipkin-Meshkov-Glick Hamiltonian from nuclear physics [3–6], and the Dicke model from quantum optics [7–9].

The high degree of similarity between the behavior of these systems suggests an underlying universality, and in this paper we explore this universality in terms of a quantum mechanical catastrophe theory.

In its elementary, classical form, catastrophe theory is the study of the critical points of potentials, with emphasis on a qualitative understanding of the properties of the system as critical points are born, move about, merge, and disappear as control parameters are varied [10]. The best known catastrophe is the *cusp*, which describes the bifurcation of a critical point. The relation between entanglement properties and the cusp has been noted previously for the Dicke model [7], and the importance of bifurcations in the appearance of entanglement maxima has been conjectured as a general rule [11,12]. In this paper, we shall explore and expand upon these ideas.

Some properties of the quantum cusp have been discussed by Gilmore *et al.* [13] but our focus here is different, and the way in which we obtain a quantum model from the classical catastrophe differs accordingly. The method employed here admits the concept of a macroscopic or semiclassical limit; thus establishing the connexion with models of quantum phase transitions (QPT). The quantum cusp model we construct may be thought of as a minimal model that exhibits the salient entanglement features observed in these models. We study not only the cusp, but two further catastrophes—the butterfly and a two-dimensional example—the entanglement properties of which expand upon the types of behavior one might expect in more realistic models.

*Present address: Department of Physics, University of California San Diego, La Jolla, California 92093-0319.

II. QUANTUM CATASTROPHE MODELS

We begin by constructing the quantum catastrophe models and first consider those derived from catastrophes occurring in a single variable, such as the cusp.

We take as our model a system of two interacting bosonic modes. Let (x_1, p_{x_1}) and (x_2, p_{x_2}) be the (abstract) position and momentum coordinates representing these modes. We assume an interaction between these modes such that the interacting system is separable in a description in terms of two *collective* bosonic excitations, the coordinates of which we denote (y_1, p_{y_1}) and (y_2, p_{y_2}). We construct the Hamiltonian of one of these collective modes y_1 so that it undergoes the catastrophe. The question that we shall address is then: Given the structure of the system in terms of the collective modes $\mathbf{y}$, what is the entanglement between the original bare modes $\mathbf{x}$?

We write the Hamiltonian of the collective mode in which the catastrophe occurs as

$$H_1 = \frac{1}{2m} p_{y_1}^2 + m\omega^2 U_{\text{cat}}(y_1) \tag{1}$$

with m and ω the characteristic mass and frequency of the mode. The potential $U_{\text{cat}}(y_1)$ is taken from elementary catastrophe theory, and can be written as a power series $U_{\text{cat}}(y) = \sum_{n=1}^{\infty} A_n y_1^n$. We rescale the coordinate $y_1 \to y_1\sqrt{\hbar/m\omega}$, and measure the energy in units $\hbar\omega$, such that

$$H_1 = -\frac{1}{2}\frac{d^2}{dy_1^2} + \sum_{n=1}^{\infty} \frac{A_n}{\mu^{n/2-1}} y_1^n = -\frac{1}{2}\frac{d^2}{dy_1^2} + V_{\text{cat}}(y_1), \tag{2}$$

which defines the rescaled catastrophe potential $V_{\text{cat}}(y_1)$. Here, $\mu \equiv m\omega/\hbar$ is our explicit "macroscopy" parameter, which is meant in the sense that the limit $\mu \to \infty$ can be thought of either as the limit in which the system size (and hence mass m) becomes macroscopic, or as the semiclassical limit $\hbar \to 0$. The limit $\mu \to \infty$ is analogous to the thermodynamic limit in the QPT models, and therein lies the correspondence between these quantum catastrophes and the QPT work cited in the Introduction.

The behavior of the mode described by the H_1 is largely governed by the fixed points of the classical catastrophe potential $V_{\mathrm{cat}}(y_1)$, and this is especially true in the limit $\mu\to\infty$. By construction the fixed points of $V_{\mathrm{cat}}(y_1)$, which we denote $\tilde{y}$, are of the order $\tilde{y}\sim\sqrt{\mu}$, and are thus "macroscopic." Expanding $V_{\mathrm{cat}}(y_1)$ in Eq. (2) about $\tilde{y}$ and taking the limit $\mu\to\infty$ we obtain

$$\tilde{H} = -\frac{1}{2}\frac{d^2}{dy_1^2} + \frac{1}{2}\left.\frac{d^2V}{dy_1^2}\right|_{y_1=\tilde{y}} y_1^2 + V(\tilde{y}). \tag{3}$$

This effective Hamiltonian describes small $O(1)$ fluctuations about fixed point $\tilde{y}$. The second derivative determines the excitation spectrum around the fixed point, and $V(\tilde{y})\sim O(\mu)$ is the energy of the bottom of the harmonic potential well in which the system is localized. In general, the potential will have more than one fixed point and an independent effective Hamiltonian may be derived for each. The way in which contributions from different fixed points combine to give the overall ground state of the quantum system will be treated for individual catastrophes.

The second collective mode y_2 is assumed to be simple harmonic, and thus the full Hamiltonian of the catastrophe model is

$$H_{\mathrm{cat}}(\mathbf{y}) = -\frac{1}{2}\frac{d^2}{dy_1^2} - \frac{1}{2}\frac{d^2}{dy_2^2} + V_{\mathrm{cat}}(y_1) + \frac{1}{2}y_2^2, \tag{4}$$

We relate the coordinates of the two collective modes $\mathbf{y}$ to those of the bare modes $\mathbf{x}$ via the rotation

$$y_1 = cx_1 + sx_2, \quad y_2 = -sx_1 + cx_2, \tag{5}$$

where $c=\cos(\theta/2)$ and $s=\sin(\theta/2)$, and θ reflects the degree of mixing. In terms of the $\mathbf{x}$-representation, $H_{\mathrm{cat}}(\mathbf{x})$ is not separable, and this rotation generates an interaction between the two bare modes $\mathbf{x}$. We quantize the collective coordinates y_i and the bare coordinates x_i according to

$$y_i = 2^{-1/2}(b_i^\dagger + b_i), \quad x_i = 2^{-1/2}(a_i^\dagger + a_i), \tag{6}$$

with momenta defined canonically. In this second quantized notation, the two representations are related through a two-mode SU(2) squeezing transformation described by the unitary operator $W=\exp(-(\theta/2)a_1^\dagger a_2+(\theta/2)a_1 a_2^\dagger)$.

To make the connexion with a familiar model: the above scheme is very similar to the Dicke model in the thermodynamic limit. Here, the two bare modes are the photon field and the collective atomic coordinate, and these are related to the collective excitations (polaritons) by just such a squeezing [14,15].

In this paper, we consider two one-dimensional catastrophes—the cuspoids A_{+3} and A_{+5}, commonly referred to as the cusp and the butterfly. We shall also consider a catastrophe that occurs in two dimensions, $V_{\mathrm{cat}}(y_1,y_2)$ and is nonseparable. In this case, we calculate the entanglement between the modes y_1 and y_2 with the catastrophe itself providing the interaction between the modes. In selecting which catastrophes to study, we require that the spectra of the catastrophe be bounded from below for all values of the control parameters at finite μ.

III. ENTANGLEMENT ABOUT FIXED POINTS: $\mu\to\infty$ LIMIT

For the one-dimensional catastrophes, the two-mode Hamiltonian that determines the excitations about $\tilde{y}_1$ in the $\mu\to\infty$ limit is

$$H = -\frac{1}{2}\frac{d^2}{dy_1^2} - \frac{1}{2}\frac{d^2}{dy_2^2} + \frac{1}{2}\epsilon_1^2 y_1^2 + \frac{1}{2}y_2^2 + V(\tilde{y}_1) \tag{7}$$

with $\epsilon_1^2 = d^2V/dy_1^2|_{y_1=\tilde{y}}$. The ground state wave function of the system is thus the Gaussian

$$\Psi(\mathbf{y}) = (\pi^2/\epsilon_1)^{-1/4}\exp\left(-\frac{\epsilon_1}{2}y_1^2 - \frac{1}{2}y_2^2\right), \tag{8}$$

which in the $\mathbf{x}$-representation reads

$$\Psi(\mathbf{x}) = \left(\frac{\pi^2}{\epsilon_1}\right)^{1/4}\exp\left\{-\frac{\epsilon_1}{2}(cx_1+sx_2)^2 - \frac{1}{2}(sx_1-cx_2)^2\right\}. \tag{9}$$

To find the entanglement of this wave function, we require the reduced density matrix (RDM) of one of the bare modes, x_1, say. This is obtained through $\rho(x_1,x_1')=\int dx_2\Psi(x_1,x_2)\Psi^*(x_1',x_2)$ as

$$\rho(x_1,x_1') = \frac{\pi}{\sqrt{\epsilon_1(s^2\epsilon_1+c^2)}}\exp\{-\alpha(x_1^2+x_1'^2)+\beta x_1x_2\}, \tag{10}$$

where α and β are coefficients, only the ratio of which is important for the entanglement:

$$\frac{2\alpha}{\beta} = \frac{(\epsilon_1+1)^2 + 2\epsilon_1[\cot^2(\theta/2)+\tan^2(\theta/2)]}{(\epsilon_1-1)^2}. \tag{11}$$

We shall quantify the entanglement in our two mode system with the von Neumann entropy S. The entropy of the density matrix $\rho(x_1,x_1')$ is evaluated by comparison with the density matrix of a harmonic oscillator at finite temperature. Details of this approach have been given elsewhere [8], and we just give the result here:

$$S = \frac{1}{\log 2}\left\{\frac{\Omega}{2T}\coth\left(\frac{\Omega}{2T}\right) - \ln\left[2\sinh\left(\frac{\Omega}{2T}\right)\right]\right\}, \tag{12}$$

where the ratio of frequency to temperature of the fictitious oscillator is given by $\Omega/T=\mathrm{arccosh}(2\alpha/\beta)$. For the one-dimensional catastrophes, the entanglement is maximized when the squeezing angle is $\theta=\pi/2$. For this choice, Eq. (11) simplifies to

$$\frac{2\alpha}{\beta} = \frac{\epsilon_1^2+6\epsilon_1+1}{(\epsilon_1-1)^2}. \tag{13}$$

This procedure is easily adapted to calculate the entanglement in the two-dimensional catastrophe.

We now consider our three example catastrophes in turn.

IV. CUSP

The cusp catastrophe, A_{+3} is the most familiar and, from the point of view of applications, the most important catastrophe. With coefficients chosen for convenience, the scaled cusp potential is

$$V_{+3}(y_1) = \frac{1}{4\mu}y_1^4 + \frac{A}{2}y_1^2. \tag{14}$$

We shall only consider a harmonic perturbation here, and reserve until later a discussion of the effects of linear perturbations. We also shall set $\theta=\pi/2$ here to give maximum mixing between the modes. This leaves us with a single control parameter A.

The full two-mode Hamiltonian in terms of the creation and annihilation operators of the $\mathbf{x}$-modes is

$$\begin{aligned} H_{+3}(\mathbf{a}) = {} & \frac{A+3}{4}(a_1^\dagger a_1 + a_2^\dagger a_2 + 1) + \frac{A-1}{8}(a_1^{\dagger 2} + a_1^2 + a_2^{\dagger 2} + a_2^2) \\ & + \frac{A-1}{4}(a_1^\dagger a_2 + a_1 a_2^\dagger + a_1^\dagger a_2^\dagger + a_1 a_2) \\ & + \frac{1}{64\mu}(a_1^\dagger + a_1 + a_2^\dagger + a_2)^4. \end{aligned} \tag{15}$$

It may at first appear unusual that the coefficient of $a_i^\dagger a_i$ should depend on the parameter A. However, it can be shown that, by individually squeezing the collective modes before applying the two-mode SU(2) transformation, this dependence on A can be removed. If both modes are squeezed identically, the entanglement properties of the system are left invariant, since this squeezing then represents a global rescaling of the phase space. For simplicity though, we retain the form of Eq. (15).

We now consider the fixed points. For $A>0$, only one stable fixed point exists and this lies at the origin. Taking $\mu\to\infty$, we see that the excitation energy about this fixed point is $\epsilon_1=\sqrt{A}$. For $A<0$, the origin becomes unstable, and two new stable fixed points appear at $y_1=\pm\sqrt{\mu|A|}$. In the $\mu\to\infty$ limit, these two fixed points are degenerate and have the same excitation energy $\epsilon_1=2\sqrt{|A|}$. The shape of the potential is sketched as insets in Fig. 1 and shows clearly the change of the potential from double to single well structure. Note that the form V_{+3}, Eq. (11), is also used in Landau theory of phase transition in statistical mechanics, or in quantum field theory (ϕ^4-model). Describing the vanishing of the excitation energy as $\epsilon_1\sim A^{z\nu}$, and the divergence of the "correlation length" as $\xi\equiv\epsilon^{-1/2}\sim A^{\nu}$, we find exponents $\nu=1/4$ and $z=2$.

We now consider the entanglement. For $A>0$, the entropy follows directly from the approach outlined in Sec. III. For $A<0$, the situation is complicated slightly by the existence of two fixed points. With the limit $\mu\to\infty$ taken in correspondence with the thermodynamic limit, the ground state of the system would be an equal mixture of density matrices localized at the two fixed points. We prefer here to use the limit $\mu\to\infty$ to calculate an approximate wave function for finite but large μ. This is obtained by taking a coherent superposition of the two localized wave functions and allows direct comparison with the numerical results for finite μ. Since the two lobes are orthogonal, the reduced density matrix of the total system is equal to the sum of the reduced density matrices for the two lobes: $\rho_1=1/2(\rho_+ + \rho_-)$. This is the same

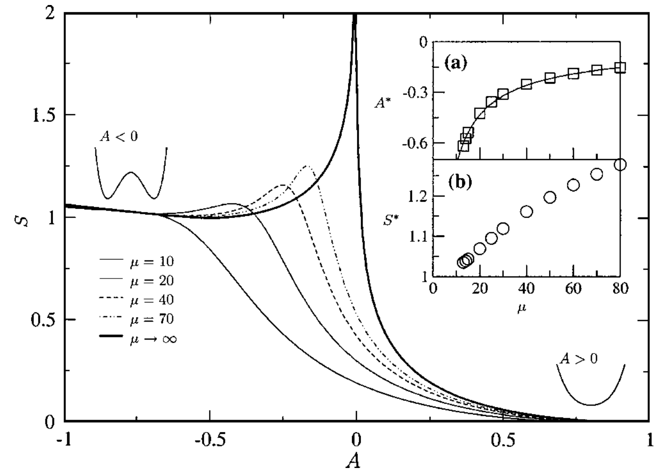

FIG. 1. Entanglement properties of the cusp catastrophe. The von Neumann entropy S in the macroscopic limit $\mu\to\infty$ (thick line) shows a divergence at the critical value $A=0$ where the potential changes from a double- to a single-well structure (inset sketches). Numerical results for finite μ show a peak near this point. Inset (a) shows the scaling with μ of the parameter value A^* at which the entanglement maximum occurs, and (b) shows the value of the entropy S^* at this point.

result as is obtained if one takes the ground-state to be the incoherent mixture; so the difference between these two approaches is unimportant. However, this will be seen not to be the case when we consider the two-dimensional catastrophe.

From the general theory of entropy [16] we know that for $\rho=\Sigma_i\lambda_i\rho_i$ with λ_i probabilities, the total entropy $S(\rho)$ is bounded by

$$\sum_i \lambda_i S(\rho_i) \leqslant S(\rho) \leqslant \sum_i \lambda_i S(\rho_i) - \lambda_i \lg \lambda_i. \tag{16}$$

In the current situation, since ρ_+ is orthogonal to ρ_-, the upper bound becomes an equality. Furthermore, since $S(\rho_+)=S(\rho_-)$, we have $S(\rho_1)=S_{\mathrm{mix}}+S(\rho_+)$ with $S_{\mathrm{mix}}=1$. The mixing entropy represents the contribution from the "global," i.e. macroscopic, structure of the wave function, whereas local structure enters through the individual $S(\rho_+)$ terms. If the parity symmetry $V_{+3}(y_1)=V_{+3}(-y_1)$ is broken by an additional linear term $\propto y_1$ in the potential, the degeneracy of the two fixed points would be lifted and the contribution from the mixing entropy $S_{\mathrm{mix}}=1$ would disappear.

The single-well entropy $S(\rho_+)$ is calculated as in Sec. III, and we plot the total entropy $S(\rho)$ in Fig. 1. The similarity between the behavior of this simple cusp model and the QPT models is apparent. At the critical point, the entropy diverges as

$$S \sim \nu \lg A = \lg \xi, \tag{17}$$

i.e., with the correlation length ξ, and we thus see "critical entanglement" [17].

Numerically obtained results for finite μ are shown alongside the $\mu\to\infty$ result. The value of A for which the peak in the entanglement occurs at finite μ, A^*, scales with μ to a very good approximation as $A^*=c\mu^{0.75}$ with a numerically determined constant of $c=4.1$. This relation is plotted in Fig. 1(a). We mention that the exponent of $0.75 \approx 3/4$ has been observed numerically for the entropy in the Dicke model [7]. We also investigated the value of the entropy S^* at its peak [Fig. 1(b)] but found no convincing scaling relation for finite μ.

V. BUTTERFLY

The second one-dimensional catastrophe that we study is the butterfly, A_{+5}, which gives rise to the potential

$$V_{+5}(y_1) = \frac{A_2}{2}y_1^2 + \frac{A_4}{4\mu}y_1^4 + \frac{1}{6\mu^2}y_1^6. \tag{18}$$

The parameter space is two-dimensional (A_2, A_4), and rather than give a full account of this space, we simply look at two representative values of A_4

Case (i): $A_4=0$. For $A_2>0$, $y_1=0$ is the only fixed point and this has excitation energy $\epsilon_1=\sqrt{A_2}$. For $A_2<0$, $\tilde{y} = \pm\sqrt{\mu}|A_2|^{1/4}$ are the two stable fixed points, both with $\epsilon_1 = \sqrt{2|A_2|}$. Apart from numerical coefficients, the behavior here is the same as that of the cusp. This result generalizes to all A_{+k} catastrophes: for V_{+k} with $A_i=0, \forall i>2$ the excitation energy is $\sqrt{A_2}$ for $A_2>0$, and $\sqrt{(k-3)|A_2|}$ for $A<0$, with behavior like that of the cusp.

Case (ii): $A_4=-4/\sqrt{3}$. Here we see new behavior absent in the cusp. The A_2 parameter range is divided up into three regions by the fixed points,

$$\begin{aligned} A_2 < 0; &\quad \tilde{y} = \pm\left[\frac{\mu}{\sqrt{3}}(2+\sqrt{4-3A_2})\right]^{1/2} \equiv \tilde{y}_\pm \\ 0 < A_2 < 4/3; &\quad \tilde{y} = 0 \\ &\quad \tilde{y} = \tilde{y}_\pm \\ A_2 > 4/3; &\quad \tilde{y} = 0. \end{aligned} \tag{19}$$

Thus, increasing A_2 from below zero upwards, the potential moves through a sequence of first a double, then triple, then single well structures, as shown by the insets in Fig. 2.

The stability or otherwise of the fixed points is only part of the story in determining the $\mu\to\infty$ ground state of the system. For $A_2>4/3$ and $A_2<0$, the situation is straightforward and the ground state is obtained exactly as for the two phases in the cusp. In the central region $0<A_2<4/3$, however, we have three fixed points, and their weight in determining the ground state depends on the energy $V(\tilde{y})$ of the bottom of the well at $\tilde{y}$. In the $\mu\to\infty$ limit, the system will be completely localized in whichever of the fixed points has the lowest base energy, or, if the energies are degenerate, we take an equal superposition to describe the large-μ wave function. For $A_2>1$, $y=0$ is the fixed point with lowest energy, and for $A_2<1$ the two fixed points at finite displacements $y=\tilde{y}_\pm$ have the lowest energy and are degenerate. Only at $A=1$ are all three points degenerate and we have a three-lobed wave function.

This structure is induced by a level crossing in the $\mu\to\infty$ spectrum, with the energy of the double well crossing

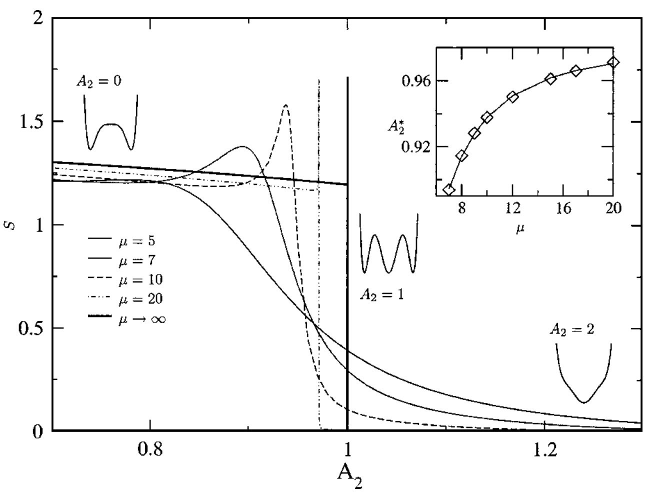

FIG. 2. The von Neumann entropy of the Butterfly catastrophe with $A_4=-4/\sqrt{3}$ as the potential undergoes a double-triple-single well transition, both for $\mu\to\infty$ and finite μ. The profile of the entanglement is very different to that of the cusp as the transition here is induced by a level crossing in the spectrum. Inset shows scaling of A_2^* as a function of μ.

the energy of the single well at $A=1$. For finite μ, the level-crossing is actually avoided, due to the overlap of all three wells. This situation therefore bears some similarity to that described in Ref. [18], where a discontinuous entanglement was observed at a level crossing associated with a first-order QPT.

Away from the level crossing, the entanglement is calculated just as for the cusp. In the region of $A_2=1$, we need to exercise a little care, because the entanglement is discontinuous at $A_2=1$. Exactly at this point, the excitation energies of the three wells do not disappear, but rather take the finite values $\epsilon_1=(1,2,2)$. The entanglement in the central well (with $\epsilon_1=1$) is zero, $S_0=0$, since the wave function is circularly symmetric about the origin ($\epsilon_2=1$ as well) and can thus be written as a product state with respect to all coordinate systems. The entanglement for each of the displaced wells is $S_\pm\approx 0.197$. Thus, by combining the appropriate density matrices, we find that for A_2 slightly less than unity, the double-well state has $S=1.197$. For A_2 just slightly bigger than unity we have $S=0$, due to the product state in the single well. Directly at $A_2=1$ we have the three-lobed wave function, and $S=2/3S_+ + 1/2S_- + \lg 3 \approx 1.716$. These results plus the corresponding finite μ data are shown in Fig. 2. The approach of the finite μ results to the $\mu\to\infty$ limit is nicely seen, and in particular to the limiting value of $S\approx 1.716$ at $A_2=1$.

We stress that the entanglement maximum occurs not at the value of A_2 at which the fixed point becomes unstable, but rather at the level crossing. Moving through the points $A_2=0$ and $A_2=4/3$, where fixed point stability does change, nothing special happens to the entropy (or any other ground-state property), since these fixed points do not contribute to the determination of the ground state at these values of A_2.

By examining the finite μ data [Fig. 2(b)], we determine that the value of A_2 at which the entanglement peak occurs scales as $A^*-1 \sim c_0\mu^{-c_1}$ with numerical parameters (c_0, c_1) determined to be $(-3.55, 1.90)$ to within a few percent.

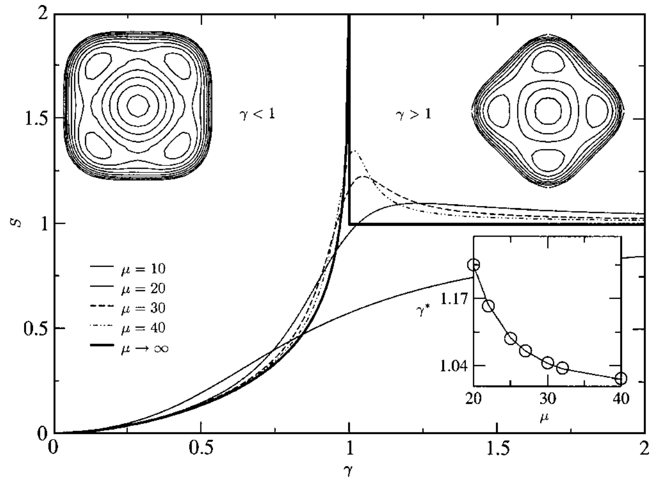

FIG. 3. The von Neumann entropy of the two-dimensional molar catastrophe with $A=-1$ as a function of γ. Plots of the potential for $\gamma<1$ and $\gamma>1$ are shown at the top of the figure. The origin of the potential is unstable and there are four stable potential wells satellite to this. Lower right inset shows scaling of γ^{*} as a function of μ.

VI. TWO-DIMENSIONAL CATASTROPHE

The most familiar two-dimensional catastrophes are the umbillics with the germs $y_1^2 y_2 \pm y_2^3$. However, these are unsuitable for our purpose as their spectra are not bounded from below and this, in fact, is true of all the two-dimensional, elementary catastrophes of Thom [19]. Therefore, we consider the nonsimple catastrophe

$$V_m = \frac{1}{2}A(y_1^2 + y_2^2) + \frac{1}{4\mu}(y_1^4 + 2\gamma y_1^2 y_2^2 + y_2^4), \qquad (20)$$

where we have only included harmonic perturbations as before. This catastrophe is described as nonsimple because the germ (that part proportional to μ^{-1} in the above) depends irreducibly on a modulus, γ, whereas simple germs have no free parameters.

The fixed point structure of V_m divides the behavior into three regimes in the $\mu\to\infty$ limit. For $A>0$, we obtain a single fixed point at the origin, and since the ground-state of the system is a product state of two Gaussians with the same width, there is no entanglement. For $A<0$, the origin is unstable; for $\gamma\neq 1$, the system possesses four fixed points, as is readily observed from the molar-shaped potentials plotted as insets of Fig. 3. For all $\gamma>1$, the four stable fixed points lie on the lines $y_1=0$ and $y_2=0$, whereas for $\gamma<1$ they lie on the diagonals $y_1=\pm y_2$. In the following, we set $A_2=-1$ throughout, as the entanglement properties are the same for all $A_2<0$. We calculate the entanglement between modes y_1 and y_2 induced by the interaction in the catastrophe itself, and do not apply the two-mode squeezing.

We first study $\gamma>1$ as this is the simpler of the two cases. The stable fixed points are given by

$$(y_1,y_2) = (\pm\sqrt{\mu},0); \quad (y_1,y_2) = (0,\pm\sqrt{\mu}). \qquad (21)$$

At each fixed point, y_1 and y_2 are the excitation coordinates with excitation energies

$$\epsilon_+^2 = 2; \quad \epsilon_-^2 = \gamma - 1. \qquad (22)$$

Excitations in the direction of the displacement $\pm\sqrt{\mu}$ are described ϵ_+.

The individual wave functions localized around any of these fixed points are unentangled, since they are just products of Gaussians is the y_1 and y_2 directions. However, combining these four functions into the four-lobed wave function that describes the large μ limit, the total system is entangled. This is solely due to the mixing entropy of its four lobed structure.

We can not calculate the entanglement of this structure in the way we did for the one-dimensional catastrophes, because the four reduced density matrices of each lobe are not orthogonal. This means that the upper bound in Eq. (16) remains as an upper bound, and is not equality. Nevertheless, we can proceed as follows. Writing $|\tilde{y}_1,\tilde{y}_2\rangle$ for the wave function of the system localized at $(\tilde{y}_1,\tilde{y}_2)$, the four-lobed large-$\mu$ wave function can be written as

$$|\Psi\rangle = \tfrac{1}{2}\{|\tilde{y},0\rangle + |-\tilde{y},0\rangle + |0,\tilde{y}\rangle + |0,-\tilde{y}\rangle\} \qquad (23)$$

with $\tilde{y}=\sqrt{\mu}$. Given that the individual lobes contribute nothing to the entanglement by themselves, we ignore their individual structure in this description. In the limit $\mu\to\infty$, the three single-mode states $|0\rangle$, $|\pm\tilde{y}\rangle$ are all orthogonal, and thus the RDM of one of the modes $\rho_1=\mathrm{Tr}_2|\Psi\rangle\langle\Psi|$ is

$$\rho_1 = \tfrac{1}{4}\{(|\tilde{y}\rangle + |-\tilde{y}\rangle)(\langle\tilde{y}| + \langle-\tilde{y}|) + 2|0\rangle\langle 0|\}. \qquad (24)$$

Furthermore, the orthogonality of these states means that this density matrix can be simply treated as a three-by-three matrix and the entropy is simply $S=1$, independent of γ for $\gamma>1$.

It is interesting to note that had we taken as the ground-state density matrix the incoherent mixture of the four contributions,

$$\rho = \tfrac{1}{4}\{|\tilde{y},0\rangle\langle\tilde{y},0| + |-\tilde{y},0\rangle\langle-\tilde{y},0| + |0,\tilde{y}\rangle\langle 0,\tilde{y}| + |0,-\tilde{y}\rangle\langle 0,-\tilde{y}|\}, \qquad (25)$$

leading to the RDM

$$\rho_1 = \tfrac{1}{4}\{|\tilde{y}\rangle\langle\tilde{y}| + |-\tilde{y}\rangle\langle-\tilde{y}| + 2|0\rangle\langle 0|\} \qquad (26)$$

and a value of the von Neumann entropy of $S=3/2$, which is clearly at variance with the numerical results.

We now consider the region $\gamma<1$, and for simplicity we also assume $\gamma>0$. The four fixed points are

$$(y_1,y_2) = \left(\pm\sqrt{\frac{\mu}{1+\gamma}}, \pm\sqrt{\frac{\mu}{1+\gamma}}\right) \qquad (27)$$

where the two $\pm$ signs are independent. Each fixed point has the excitation energies

$$\epsilon_+^2 = 2; \quad \epsilon_-^2 = 2\frac{1-\gamma}{1+\gamma}. \qquad (28)$$

The eigenmodes of the system are not y_1 and y_2, but rather lie along, and perpendicular to, the diagonals of the y_1-y_2 plane. Each individual fixed-point wave function is thus entangled with respect to modes y_1 and y_2.

This entanglement can be calculated as in Sec. III, but here with two excitation energies and the rotation between the eigenmodes and the **y** coordinates. The entanglement determining parameter $2\alpha/\beta$ is evaluated to be

$$\frac{2\alpha}{\beta} = \frac{4 - 3\gamma^2 + 4\sqrt{1-\gamma^2}}{\gamma^2}, \tag{29}$$

from which the single-lobe entanglement follows directly.

The contribution of the four-lobed structure of the large-μ superposition can be assessed as follows. From a macroscopic point of view, we can ignore the structure of the individual lobes, and write the wave function as

$$\begin{aligned} |\Psi\rangle &= \tfrac{1}{2}\{|\tilde{y},\tilde{y}\rangle + |\tilde{y}-,\tilde{y}\rangle + |-\tilde{y},\tilde{y}\rangle + |-\tilde{y},-\tilde{y}\rangle\} \\ &= \tfrac{1}{2}(|\tilde{y}\rangle + |-\tilde{y}\rangle) \otimes (|\tilde{y}\rangle + |-\tilde{y}\rangle). \end{aligned} \tag{30}$$

The second forms clearly shows this wave function to be a product state from the macroscopic viewpoint. Thus the mixing entropy of forming the four-lobed structure is zero, and the entropy of the system is just the single lobe entropy above.

In Fig. 3 we plot these results alongside the numerical data for finite μ. The scaling of γ^* with μ is observed to be $\gamma^* - 1 = c_0\mu^{-c_1}$ with coefficients fitted as $(c_0, c_1) = (4.93 \times 10^4, 4.09)$.

VII. CONCLUSIONS

We have constructed and studied a family of quantum catastrophe models, and investigated their ground-state entanglement properties. The cusp catastrophe, with its bifurcating fixed point, demonstrates behavior that is remarkably similar to the QPT models, such as the Dicke model—underlining the importance of bifurcations of classical fixed points in this context. It should be noted that while this bifurcation occurs for all values of μ, a peak in the entanglement is only observed when μ is sufficiently large ($\mu > 10$ here). This illustrates that the bifurcation is not, in itself, a sufficient condition for the occurrence of the entanglement maximum, but that the system must also be capable of sufficient delocalization. The butterfly catastrophe displays very different behavior to the cusp, namely, a discontinuous entropy induced by a level crossing in the macroscopic limit.

The cusp and the two-dimensional catastrophe demonstrate that a mixing term in the entropy can contribute to the total entanglement in cases where a wave function is split up into localization areas that are separated within (abstract) position space. In particular the two-dimensional catastrophe suggests a distinction between "global" and "local" (within the lobes) entanglement, and one could speculate that in more complex situations, with wave functions split up further and further, a hierarchy of entanglement entropies might emerge.

Our results also have a bearing on the issue of quantum chaos and entanglement in such systems, as the one-dimensional models studied here are capable of emulating the behavior of more sophisticated nonlinear Hamiltonians, despite being separable, and thus integrable. It is clear that there is no unequivocal relation between delocalization and the onset of quantum chaos on one hand and the peaking of entanglement on the other.

ACKNOWLEDGMENT

This work was supported by the Dutch Science Foundation NWO/FOM and the UK EPSRC Network "Transport, Dissipation, and Control in Quantum Devices."

[1] A. Osterloh, L. Amico, G. Falci, and R. Fazio, Nature (London) **416**, 608 (2002).
[2] S. Schneider and G. J. Milburn, Phys. Rev. A **65**, 042107 (2002).
[3] H. J. Lipkin, N. Meshkov, and A. Glick, Nucl. Phys. **62**, 188 (1965).
[4] J. Vidal, G. Palacios, and R. Mosseri, Phys. Rev. A **69**, 022107 (2004).
[5] S. Dusuel and J. Vidal, Phys. Rev. Lett. **93**, 237204 (2004).
[6] J. I. Latorre, R. Orús, E. Rico, and J. Vidal, cond-mat/0409611 (2004).
[7] N. Lambert, C. Emary, and T. Brandes, Phys. Rev. Lett. **92**, 073602 (2004).
[8] N. Lambert, C. Emary, and T. Brandes, Phys. Rev. A **71**, 053804 (2005).
[9] J. Reslen, L. Quiroga, and N. F. Johnson, Europhys. Lett. **69**, 8 (2005).
[10] R. Gilmore, *Catastrophe Theory for Scientists and Engineers* (Wiley, New York, 1981).
[11] A. P. Hines, G. J. Milburn, and R. H. McKenzie, quant-ph/0308165 (2003).
[12] A. P. Hines, C. M. Dawson, R. H. McKenzie, and G. J. Milburn, Phys. Rev. A **70**, 022303 (2004).
[13] R. Gilmore, S. Kais, and R. D. Levine, Phys. Rev. A **34**, 2442 (1986).
[14] C. Emary and T. Brandes, Phys. Rev. Lett. **90**, 044101 (2003); Phys. Rev. E **67**, 066203 (2003).
[15] A degree of single-mode squeezing is also required in the superradiant phase of the Dicke model.
[16] A. Wehrl, Rev. Mod. Phys. **50**, 221 (1978).
[17] T. J. Osbourne and M. A. Nielsen, Phys. Rev. A **66**, 032110 (2002).
[18] J. Vidal, R. Mosseri, and J. Dukelsky, Phys. Rev. A **69**, 054101 (2004).
[19] R. Thom, *Stabilité Structurelle et Morphogénèse* (InterEditions, Paris, 1972).